BULLETIN

OF THE

KOREAN CHEMICAL SOCIETY

ISSN 0253-2964
Volume 21, Number 1

BKCSDE 21(1) 1-150
January 20, 2000

Feature Article

Electronic Spectroscopy and Structure of ClF

Vadim A. Alekseev and D. W. Setser*,†

Photonics Department, Institute of Physics, St. Petersburg State University, 198904 St. Petersburg, Russia
†Kansas State University, Department of Chemistry, Manhattan, KS USA 66506

Received December 21, 1999

Optical-optical double resonance experiments have been used to identify and characterize five ion-pair states and several of the bound and repulsive valence states of ClF. This report provides a description of these experiments for ^{35}ClF and ^{37}ClF, and a summary of the current knowledge of the valence and ion-pair states. The important role of perturbations among the rovibronic levels of the bound valence states and their utilization in the double resonance technique is discussed. The ion-pair states of the same symmetry, $\Omega=0^+$ (E and f) and 1 (β and G) interact very strongly and the spectroscopy of these states is anomalous and, hence, interesting. Comparison is made to some recent *ab initio* calculations for ClF. One possible explanation of the irregular vibrational energy levels and rotational constants of the ion-pair states of 0$^+$ and 1 symmetry is a crossing of the diabatic potentials of these states. Some currently unresolved questions about ClF spectroscopy are posed for future work. Where appropriate, analogy is made between the electronic states of ClF and the corresponding valence and ion-pair states of Cl_2.

Introduction

Until recently ClF, chlorine monofluoride, was the least studied among the halogen or interhalogen molecules from a spectroscopic point of view.[1-3] We undertook a systematic study of the excited electronic states of this molecule using methods of optical-optical double resonance (OODR) and classical emission spectroscopy.[4-7] This study revealed interesting features about the electronic structure of ClF that had not been observed previously in other halogens. In particular, strong homogeneous interactions between the $\Omega=0^+$ and 1 ion-pair states give an unusual pattern to the vibrational energy levels and rotational constants. The electronic states of ClF have been treated recently by *ab initio* calculations with inclusion of spin-orbit interactions;[8,9] and these new calculations complement the experimental results. Calculations for just the singlet ClF states had been reported earlier.[10] Although more has to be done to obtain a complete picture of the electronic states of ClF and the electronic structure of this molecule as a whole, it seems useful to present a summary of the main results of our studies and to outline the optical-optical double resonance method used to acquire the experimental data. In addition to providing a summary for ClF, comparison will be made to the valence and ion-pair states of the Cl_2 molecule in this report. Such a comparison is useful because the bond dissociation energies of the ground states are similar ($D(ClF)^{[11]}$ = 21,108 cm^{-1} and $D(Cl_2)$=19,997 cm^{-1}) and because the first set of Cl_2 and ClF ion-pair states correlate to nearly the same energy limit, $Cl^+ + Cl^-$ (or F^-), since the electron affinities of Cl (3.615 eV) and F (3.399 eV) are similar. One significant difference to be remembered is the shorter bond length for ClF (1.628 Å) *vs.* Cl_2 (1.987 Å).

The electronic states of the halogen molecules form three distinctive groups: valence, ion-pair and Rydberg states. Twenty-three valence states correlate to the $Cl(^2P_J) + F(^2P_J)$, J = 1/2 or 3/2, asympotic limits.[1] Only four of those states, $X(^1\Sigma_0^+)$, $A'(^3\Pi_2)$, $A(^3\Pi_1)$ and $B(^3\Pi_{0^+})$, are strongly bound. All three $^3\Pi$ states arise from the $\sigma^2\pi^4\pi^{*3}\sigma^{*1}$ molecular orbital configuration; we will employ the convenient shorthand notation 2431 to designate this configuration, and the same notation will be used for other molecular orbital (MO) configurations. Analogy[12] with Cl_2 and results of the calculations[8] gives reason to believe that the fourth state of the $^3\Pi$ cluster, $1(^3\Pi_{0^-})$, could be bound too, although the absence any direct observation of this state leaves this prop-

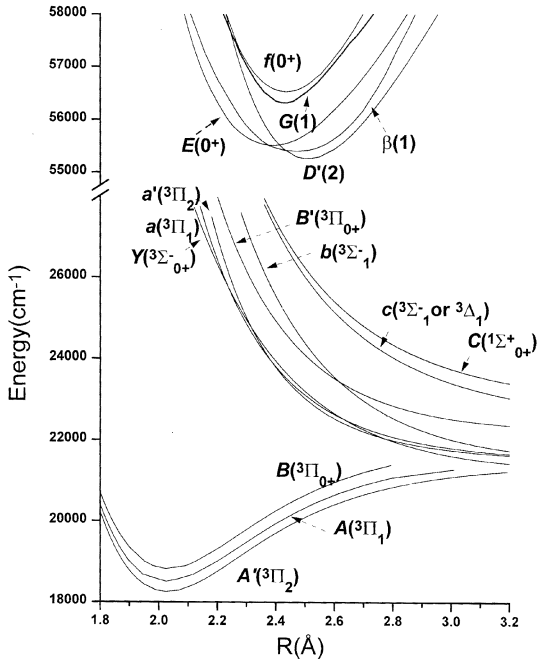

Figure 1. Potential curves for the excited states of ClF. The D', A', A and B potentials are RKR curves calculated using spectroscopic constants from Refs. 6 and 7. The potential curves for the repulsive $\Omega = 0^-$, 1 and 2 states and for the homogeneously perturbed $\Omega = 0^-$ and 1 ion-pair states were deduced from fitting bound-bound and bound-free emission spectra (see text for details). Note that R_e (1.658 Å) for ClF (X) is less than the left-hand limit of the distance scale.

osition open. Several of the bound and repulsive potentials for the valence states of ClF to be discussed are shown in Figure 1 to aid the reader.

The next group of states is the ion-pair states, which arise from the separated states of the ions. Six of the lowest in energy ion-pair states correlate to $Cl^+(^3P_{J=0,1,2}) + F(^1S_0)$. Adopting the letter code assignment of ion-pair states used in literature for other interhalogens, those six states in Hund's case c notation are:

$$F^-(^1S_0) + Cl^+(^3P_2) = D'(2), \beta(1), E(0^-)$$
$$F^-(^1S_0) + Cl^+(^3P_1) = G(1), (0^-)$$
$$F^-(^1S_0) + Cl^+(^3P_0) = f(0^+)$$

The numbers in parenthesis are the Ω values, the 0 state has no letter assignment. Owing to small spin-orbit splitting in Cl^+ (the multiplet is inverted with energies of 697 and 996 for $J = 1$ and 0, respectively), and to the similarity of the potentials for ion-pair states, the T_e values of these six ClF ion-pair states lie within ~1000 cm^{-1}. The next group of ion-pair states, which correlate to $Cl^+(^1D_2) + F^-$, lie much higher in energy, $E(^1D_2) - E(^3P_2) = 11{,}653.6$ cm^{-1}. No experimental results are available for this second group of ion-pair states at the present time. One additional ion-pair state correlates to $Cl^-(^1S_0) + F^+$. Since the $E(^1S_0) - E(^3P_2)$ energy difference for Cl^+ is 27,828 cm^{-1}, this state is rather isolated. Another set of ion-pair states correlates to $F^+ + Cl^-$, which lies 33,820 cm^{-1} above the $Cl^+(^3P) + F(^1S_0)$ asymptote. The thresholds for predissociation $Cl(4s^{2,4}P) + Cl(^2P_{3/2})$ are at 71,954 and 74,221 cm^{-1}, and all of these ion-pair states should be stable to predissociation. An interesting difference, relative to the ion-pair states of Cl_2, is that one-half of the ClF states correlate to $F^+ + Cl^-$. This group of states is, thus, at much higher energy than the states of Cl_2 with ungerade symmetry. On the other hand, the six low energy ion-pair states of Cl_2 with gerade symmetry provide an interesting reference for the Cl^+F^- states.

At one time, transitions from the lowest energy ion-pair state, $D'(2)$, to the $A'(^3\Pi_2)$ valence state of the halogen and interhalogen molecules were actively considered for possible discharge pumped ultraviolet laser applications.[13-15] The D'-A' transition for ClF is at 284 nm. Although the UV absorption spectrum of ClF extends to this wavelength, Cl_2 and F_2 mixtures have been used successfully in the laser, and 25 mJ output has been obtained from a TEA type discharge device.[14] These electrically pumped halogen systems seem to offer little advantage over the commercially developed, electrically driven, rare gas halide lasers, and current interest in ultraviolet laser applications for ClF and other halogens seems to be dormant.

The Rydberg states of ClF are the next distinctive group of states. To the best of our knowledge, the study by Alberti *et al.*[16] is the only work devoted to Rydberg states of ClF. These $4s^{1,3}\Pi$ states at ~72,000 cm^{-1}, which are above the energy range covered by the present review, correlate to various states of excited Cl atoms. According to the *ab initio* calculations,[10] the interaction of Rydberg and ion-pair states of the same symmetry should result in double-welled potentials. Such potentials have been extensively studied for Cl_2 both experimentally[17,18] and theoretically.[19] As the higher energy range of the ClF molecule becomes studied, very interesting consequences from interactions between the inner wall of the ion-pair potentials and the outer limb of the Rydberg state potentials can be anticipated.

In the present report, 5 members of the first set of ion-pair states of ClF will be discussed. In addition, the bound $A'(^3\Pi_2)$ and $A(^3\Pi_1)$ states and potentials for several of the repulsive valence states will be summarized. Numerous perturbations between rotational levels of the $B(^3\Pi_{0^+})$ and $A(^3\Pi_1)$ states facilitate excitation to ion-pair states that otherwise would be forbidden using the double resonance technique. The experiments using these perturbed levels will be emphasized in the presentation. The strong homogenous interactions between the two pairs of $\Omega = 0^-$ and the $\Omega = 1$ ion-pair states will be further documented by presentation of some ^{37}ClF data, plus extending the measurements of vibrational energies and rotational constants to higher v levels of ^{35}ClF. The recent *ab initio* calculations with spin-orbit interactions[8,9] provide a framework for an improved understanding of these four states.

Experimental Methods

In our laboratory the spectroscopy of ClF was studied by the OODR method; these results were augmented by conventional high resolution data from Tellinghuisen's labora-

tory. The OODR method is a powerful method for study of the electronic structure of halogen molecules for two reasons. Firstly, it provides a way to access excited states with much larger R_e than the ground state *via* a more weakly bound intermediate state. Secondly, the spectra are greatly simplified because individual rotational levels of the ion-pair potentials can be probed one at a time from selected levels of the intermediate state. Two separate lasers are used in the experiment. The first laser, called the pump laser, normally is used to excite molecules to a single rotational level of the bound valence states, $B(^3\Pi_{0^+})$ or $A(^3\Pi_1)$. The second laser, called the probe laser, is used to search for optical resonances between the intermediate level and the ion-pair states. In our laboratory, two Lambda Physik dye lasers were pumped by a single excimer laser to provide the pump and probe laser beams. The gas cell was fabricated from stainless-steel and was of standard design for laser-induced fluorescence experiments. The cell was passivated prior to use. The extensive OODR studies[12,20-23] of the ion-pair states of Cl_2 and Br_2 by a Japanese laboratory also illustrate the utility of the method. One advantage of using the $A(^3\Pi_1)$ state as the intermediate is that both *e*- and *f*-components of the $\Omega = 1$ ion-pair states can be explicitly probed.[20] OODR experiments have employed coherent two-photon excitation in the probe step to circumvent the $u \rightarrow g$ selection rule.[22b] Investigators also have used repulsive valence states as the intermediate state for sequential two-photon absorption.[18] Thus, the basic pump-probe, two-color excitation experiment can be used with several variations to investigate the ion-pair states of halogens.[3]

The $A \leftarrow X$ transition in ClF seems to be extremely weak due to the small spin-orbit interaction, and only the *B* state[24,25] has been an effective doorway to the ion-pair states. Transitions from the valence states of halogens to the ion-pair states, being charge transfer transition along the internuclear axis, follow very strictly the $\Delta\Omega = 0$ rule, and only the $E(0^+)$ and $f(0^-)$ ion-pair states, can be directly probed from the $B(^3\Pi_{0^+})$ state. Fortunately for these OODR experiments, a few rovibronic levels of the *B* state are perturbed by those of the $A(^3\Pi_1)$ state, which adds some $\Omega = 1$ character to the nominal *B* rovibronic levels. A summary of the currently known valence state perturbations for ClF is given in Table 1. Those *B*~*A* mixed rotational levels were used as a doorway to the ion-pair states of $\Omega = 1$ character. A typical excitation OODR spectrum is presented in Figure 2a. It displays a sequence of *P*-*R* doublets for transitions to v′, $J'-J''\perp 1 \leftarrow B(v'', J'')$ for both *E* and *f* states. The experiment must be repeated several times with different J'' levels to collect enough data for derivation of accurate spectroscopic constants. This spectrum illustrates the advantage of the OODR technique to select a single rotational level in a given vibrational level of the $B(^3\Pi_{0^+})$ state for further excitation. For some experiments, rotational relaxation within a vibrational level of the *B* state via collisions with He were deliberately used to generate a population in a range of rotational levels to accelerate the data acquisition; see Figure 2b. A typical mixture for recording such excitation spectra consisted of ClF (1-3 Torr), He (~50 Torr), and Xe (~10 Torr). The role of Xe was to provide a monitor for the ClF ion-pair states using the reactive quenching reaction to generate XeCl (*B*, *C*)

Table 1. Heterogeneous Perturbations in the *A*′, *A* and *B* States of ClF[a]

Analyzed Level	Perturbing Level	J^b	ΔE (cm^{-1})[c]	W (cm^{-1})
B(6)	*A*(8)	45-46	69(9)	0.0396(18)
B(7)	*A*(9)	14	7.53(3)	0.0433(4)
B(7)[d]	*A*(9)	16	8.9(5)	0.0422(10)
B(8)	*e*	27	47(31)	0.030(9)
B(9)	*f*	10		
A(5)	*A*′(6)	33-34	11.79(12)	0.0133(9)
A′(6)[e]	*A*(5)	33-34	-11.89(7)	0.0151(4)
B(9)	*F*(0$^+$)	≥ 21	Predissociation	
B(10)	*F*(0$^+$)	≥ 13	Predissociation	

[a]All results[7] for $^{35}Cl^{19}F$ except as otherwise indicated. Standard errors in parentheses, in terms of final digits. [b]Rotational level(s) of maximal mixing. [c]Displacement of perturbing level relative to analyzed level. [d]For $^{37}Cl^{19}F$. [e]Perturbing state uncertain: $B_e = 0.197(42)$ cm^{-1} for assumed D_e 6.6×10^{-6} cm^{-1}, H_e -6.68×10^{-6} cm^{-1}. [f]Perturbing state unknown: displacement observed in only one *J* level; this perturbation facilitated pumping to the *D*′(v′) levels. [g]From the D′→A′ emission spectrum (6), reanalyzed using current values of B_e, D_e and H_e for A(5).

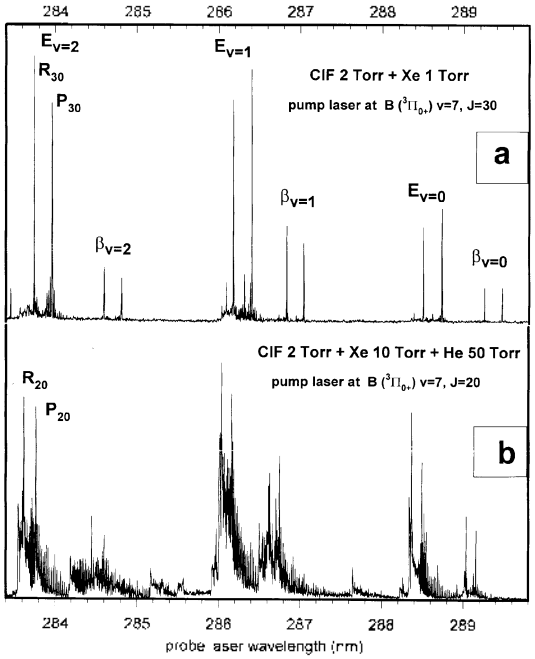

Figure 2. (a) Low resolution (0.5 nm) OODR excitation spectrum from a mixture of ClF (1 Torr) + Xe (1 Torr). The ion-pair states were detected from the XeCl (*B*-*X*) emission at 308 nm. (b) Low resolution OODR excitation spectrum from a mixture of ClF (1 Torr) − Xe (10 Torr) − He (50 Torr). The extended rotational structure demonstrates rotational relaxation within *B*(7). The weak bands marked with the asterisk are from the *B*(6) and *B*(8) vibrational levels that were populated by vibrational relaxation. The excitation of the $\beta(1)$ bands is facilitated by the heterogeneous interaction with $F(0^-)$; see the text. [Reproduced by permission from the *Journal of Chemical Physics*].

$$Cl^1F + Xe \rightarrow XeCl\,(B, C) + F$$

The competing product channel, XeF (B, C) + Cl formation, exists but the product branching ratio strongly (factor of 3) favors $XeCl^*$ over XeF^*. The XeCl (B) state, which gives strong fluorescence in the 308 nm range where the scattered laser light intensity was low, provided an excellent monitor to obtain excitation spectra of the ion-pair states. In other experiments, direct fluorescence from the ion-pair state back to the ClF (B, A or A') states was observed with a monochromator to obtain excitation spectra. The use of Xe gave more signal because the Cl^1F fluorescence spectra have broad vibrational progressions. A typical low resolution excitation spectrum ClF (E and β, $v' - 0$-2 $\leftarrow$ B, 7) obtained using the emission from XeCl (B) as the monitor is shown in Figure 2b; examples of high resolution spectra will be presented later. During the final stages of our experiments, a fortuitous three-state perturbation (B-A-A') was found that facilitated OODR excitation of $D'(2)$. The Japanese group also found an A'-A perturbation that enabled them to study $Cl_2(D')$ by the OODR method.[21b]

Low resolution, laser-induced fluorescence spectra from the Cl^1F states were acquired by removing Xe and He from the mixture. Since the radiative lifetimes of these Cl^1F states are less than ~20 ns, collisionally induced vibrational and/or electronic relaxation was not a serious problem. For our work, spectra were acquired with a 0.5 m monochromator, although the emission intensity was sufficient that higher resolution spectra could have been acquired. This fluorescence spectra was very useful, because we could selectively observe bound-bound transitions to the B, A, and A' valence states and bound-free transitions to $\Omega - 0^+$, 1 and 2 repulsive states from individually selected vibrational-rotational levels of the five ion-pair states.

High resolution emission spectra were produced and recorded at Vanderbilt University using methods very much like earlier studies of halogen spectroscopy by Tellinghuisen.[26] The excitation source was a Tesla coil discharge operated in a 7 mm-od silica tube, viewed end-on by a spectrometer. The discharge mixture contained 1-3 Torr of ClF and 200-400 Torr of Ar. Due to the decomposition of ClF by the discharge and reaction with walls of the silica tube, the ClF/Ar mixture was flowed through the discharge cell. In a static arrangement, the ClF emission intensity would rapidly drop by two orders of magnitude. Spectra were photographed at 33 Å intervals over the 2650-2900 Å region with a resolving power of 1.5×10^5. The spectra were measured using the procedures developed by Tellinghuisen.[26] A more detailed description of the experimental methods can be found in Refs. 6 and 7.

Results and Discussion

$E(0^+)$ and $f(0^+)$ ion-pair states. The search for $Cl^1F \leftarrow ClF$ (B) resonances began in the $h\nu_{pump} + h\nu_{probe}$ ~55000-62000 cm^{-1} range. The $E/f \leftarrow B$ transitions are allowed by selection rules and any suitable rovibronic level of the B state can be used for access to the E and f states. Experiments were performed in several steps. First, a low resolution fluorescence excitation spectrum, such as shown in Figure 2a, was taken to identify the resonances. Then a high resolution, high pressure spectrum was taken for each band to deduce the rotationless energy (band origin) and to assign the rotational constants. Some typical higher resolution spectra are shown in Figure 3. Because of strong interactions between the E and f states, the vibrational energy spacings were irregular (Figure 4) and the numbering of the vibrational levels was initially difficult to assign. The homogeneous interaction between E and f levels also leads to erratic values of the rotational constants *vs.* vibrational quantum number (Figure 5a), and the rotational constants for the pair of $\Omega - 0^-$ ion-pair states displayed no systematic difference. At the first stage of our work,[4] we relied upon the intensity modulation in the vibrational progressions of the ($E, f \rightarrow B$, v'') fluorescence spectra for assignment of the quantum numbers to the vibrational levels. Isotopic shift data for ^{35}ClF and ^{37}ClF subsequently were measured for confirmation of the original vibrational numbering (up to $v' - 5$ for $f(0^+)$ and $v' - 9$ for $E(0^+)$). The absolute uncertainty in the vibrational energies and B_v values was ± 2 cm^{-1} and $\pm 0.2\%$, respectively, in the original report.[4] The relative uncertainty in vibrational energies was 0.5 cm^{-1}. More recent extension of the data to $E(v' \geq 10)$ and $f(v' \geq 6)$ levels provided less pre-

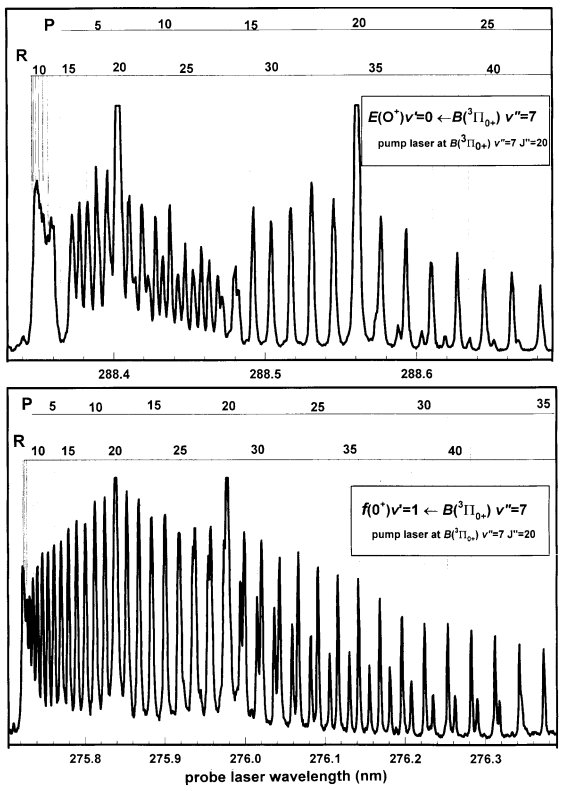

Figure 3. High resolution excitation spectra for (a) $E(0) \leftarrow B(7)$ and (b) $f(1) \leftarrow B(7)$ bands from a ClF (3 Torr) + Xe (10 Torr) + He (50 Torr) mixture. Both components of the $B(7,14)$ perturbed level are shown for the P branch by dashed lines in the top spectrum. [Reproduced by permission from the *Journal of Chemical Physics*].

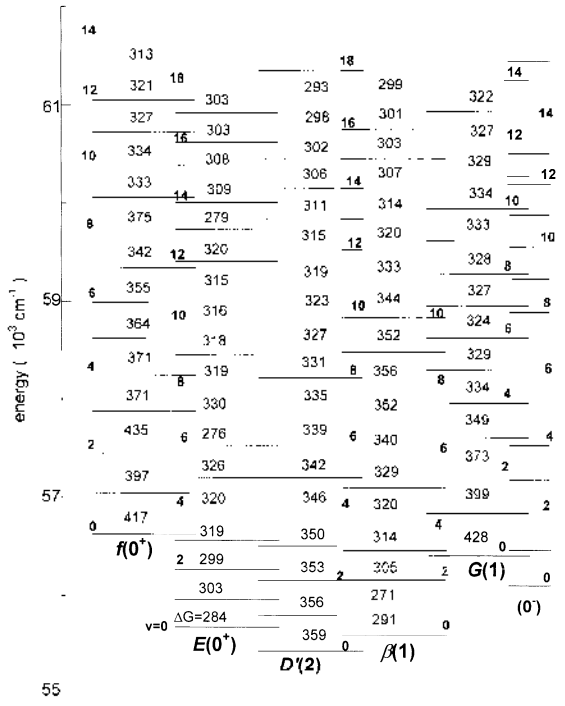

Figure 4. Schematic diagram showing the vibrational levels of the ion-pair states. The numbers between successive levels are the energy separations (cm^{-1}). The estimated positions (see text) of the levels for the 0^- state are shown on the far right side for illustration.

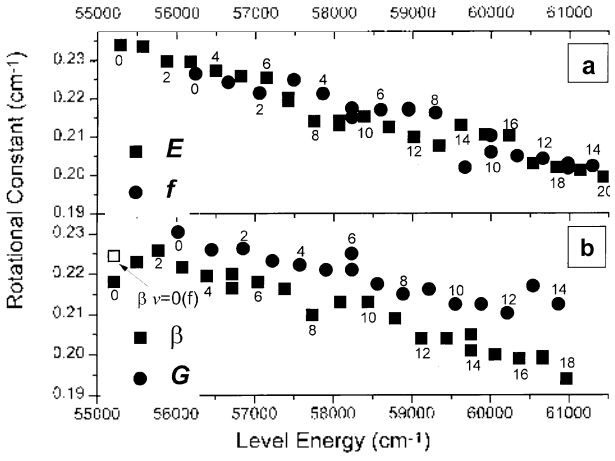

Figure 5. The rotational constants for the $\Omega=0^-$ and $\Omega=1$ ion-pair states plotted vs the total energy. The two entries for $\beta(v'=0)$ are for the (e) and (f) components. The uncertainty for the $E(v' \leq 9)$, $\beta(v'=0,1,4)$ and $f(v' \leq 5)$ levels is 0.2%. The uncertainty for the other constants is larger because only a few rotational lines in the bands were measured: the duplicate entries for multiple experiments for $f(v'=5$ and $10)$, $E(v'=9)$, $\beta(v'=5$ and $14)$ and $G(v'=6)$ illustrate the uncertainties.

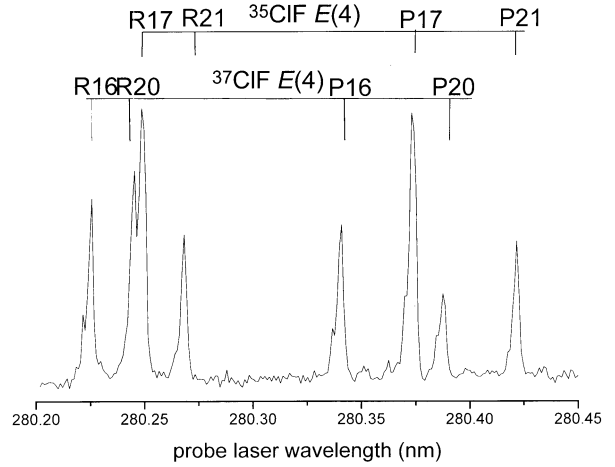

Figure 6. Excitation spectrum of the $E(4) \leftarrow B(8)$ band ^{35}ClF and ^{37}ClF. The pump laser was tuned to the ^{35}ClF($B(8,17) \leftarrow X(0,16)$), ^{35}ClF($B(8,21) \leftarrow X(0,22)$), ^{37}ClF($B(8,16) \leftarrow X(0,15)$), and ^{37}ClF($B(8,20) \leftarrow X(0,21)$) overlapped transitions: the pressure was 1 Torr of ClF.

cise values, because the data usually were taken for only two sets of P and R lines; the uncertainty in the vibrational energies and B_v values for these levels are ± 2 cm^{-1} and 1%, respectively. As shown in Figures 4 and 5, the results have been extended to $E(v'-20)$ and $f(v'-14)$. Even for these rather high v' levels, the energy spacings between the levels are not regular. In fact, a large interaction can be identified for $E(v'-13,14)$ and $f(v'-8,9)$ from the spread in energy between $v'-8$ and 9 and the compression for $v'-13$ and 14. An inversion of the B_v values also can be noted for the 7 or 8 and 12 or 13 pairs *vs.* the 9 and 14 pair.

The experiments for excitation of ^{37}ClF were performed with pure ClF at low pressure to avoid undesirable rotational relaxation or exchange of energy with ^{35}ClF molecules in the $B(^3\Pi_{0^+}; v, J)$ intermediate level. The pump laser was tuned to the ^{35}ClF($B(8,17) \leftarrow X(0,16)$), ^{35}ClF($B(8,21) \leftarrow X(0,22)$), ^{37}ClF($B(8,16) \leftarrow X(0,15)$), ^{37}ClF($B(8,20) \leftarrow X(0,21)$) overlapped transitions, which allowed us to observe two P-R doublets per band for each isotopomers of the $E, f \leftarrow B$ excitation spectra. A typical spectrum is presented in Figure 6. Using standard expression for the rotational energy, the observed lines were fitted to deduce rotational constants and vibrational energies for each level. The rotational constants obtained in this way are not precise due to the small number of lines in the excitation spectra, and we do not present the ^{37}ClF results here. Those levels of the E and f states that were not observed from excitation through $B(8)$ due to a small Frank-Condon factor were observed by pumping other rovibronic levels of the B state. The isotopic shifts for the vibrational levels of the E and f states shown in Figure 7a as a function of the total energy do serve to confirm the vibrational numbering. Two pairs of levels (f, $v'-3$ – E, $v'-7$) and (f, $v'-8$ – E, $v'-13$) show notable deviations of the isotopic shifts from the expected nearly linear dependence $\Delta E_{is}(v) \approx (1-\mu(^{35}\text{ClF})/\mu(^{37}\text{ClF}))G_{vib}(v)$ where μ is the reduced mass and $G_{vib}(v)$ is the vibrational energy of the v-th level. These results suggests strong *pairwise* homogeneous interactions between these levels, presumably because of the very close match of their unperturbed energies. On the other hand, the isotopic shifts for the remainder of the vibrational levels appear to be nearly normal to within the uncertainty of our measurements. Thus, the irregularity in the vibrational energy levels shown in Figure 4 are the same for both isotopomers. Although the energy level spacings for both E and f

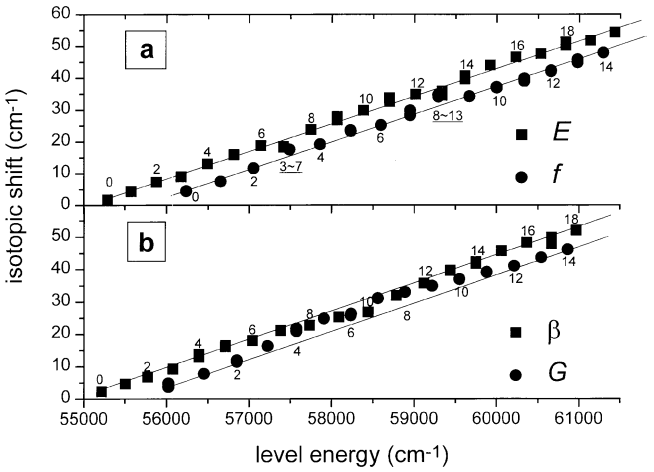

Figure 7. The isotopic shifts for the vibrational levels of the $E(0^+)$, $f(0^+)$, $\beta(1)$ and $G(1)$ states of ^{35}ClF *vs.* ^{37}ClF plotted vs total energy. The calculated isotopic shifts for the unperturbed D' state are shown by the lines for comparison.

states are irregular, the spacings between vibrational levels in the $f(0^+)$ state are always considerably larger than for levels in the $E(0^+)$ state.

The homogeneous interaction increases the isotopic shift for the f state and decreases it for the E state for all possible positions of levels relative to each other, except the case shown in Figure 8a. It easy to show that the isotopic shifts for a pair of strongly interacting levels are $\Delta E_+ - \Delta E_- - (\Delta E_1 + \Delta E_2)/2$, providing that the shift due to the interaction is much larger than the energy differences between unperturbed levels, ΔE_{12} and $\Delta E'_{12}$ (Figure 8b). The isotopic shifts for the strongly interacting pairs provide some insight into understanding the vibrational energy level pattern of the E and f states. The pairwise interactions give an estimate for the electronic part of the interaction matrix element using the

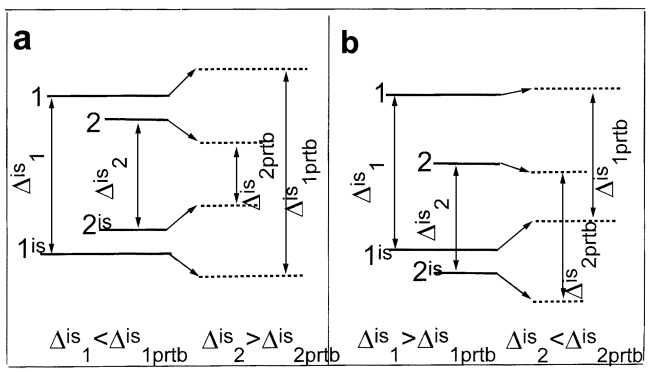

Figure 8. Schematic diagram illustrating the change of isotopic shifts due to homogeneous interactions. The positions of unperturbed and perturbed levels are shown by the solid and dashed lines, respectively. State 1 with the larger isotopic shift (higher v' level) for unperturbed level corresponds to the E state: state 2 with the smaller shift (lower v' level) corresponds to the f state. For positions of levels shown in panel (a) the homogeneous interaction results in increasing the isotopic shift for state 1 and decreasing it for state 2. For the positions of levels shown in panel (b), the homogeneous interaction leads to the opposite result.

following relation $\Delta E - 2H_e < \Psi_{v=3}|\Psi_{v=7}>$, where ΔE is the experimentally measured energy separation between $E(7)$ and $f(3)$, H_e is the electronic part of interaction and the last term is the vibrational overlap integral. If we assume that the energies of the unperturbed levels were exactly the same, then $\Delta E - 73$ cm^{-1} is entirely due to the homogeneous repulsion of the levels. If the value of the overlap integral between the $E(7)$ and $f(3)$ vibrational wavefunctions is ~0.03-0.05, the estimate for H_e is in the 700-1000 cm^{-1} range. This value may be an overestimate, but it does suggest a strong interaction.

The $\beta(1)$ and G(1) ion-pair states. The $\beta(1)$, $G(1) \leftarrow B$ transitions are optically forbidden, but the mixed $B(^3\Pi_{0^+})$ and $A(^3\Pi_1)$ rovibronic levels (see Table 1) could be used to access the β and G states. The majority of the experiments was performed using the group of perturbed rotational levels centered around $J - 14$-16 in the $B(^3\Pi_{0^+})$, $v - 7$ state. A typical spectrum in 60 Torr of He is shown in Figure 9a; only transitions from the perturbed $J - 10$-20 levels are observed. Due to the limited number of observed rotational levels, the rotational constants and vibrational energies of the $\Omega - 1$ vibrational levels were determined with poorer accuracy than for the $\Omega - 0^+$ states. However, accuracy was not our

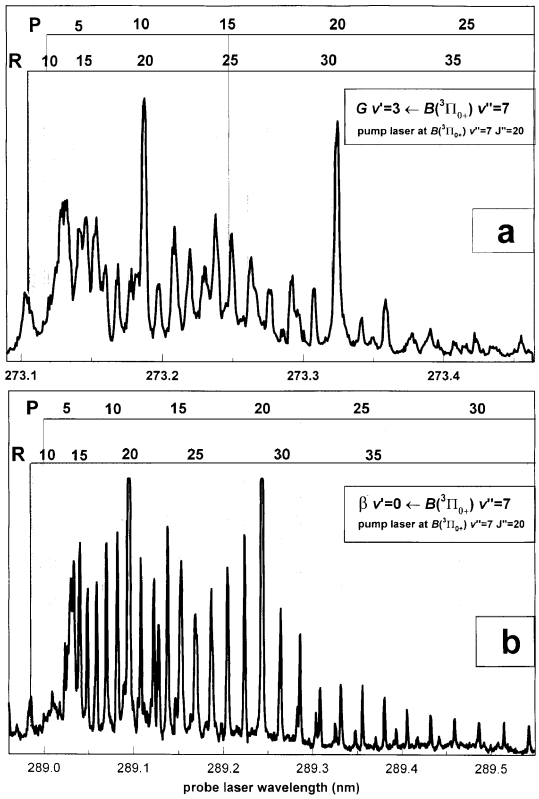

Figure 9. High resolution excitation spectra of the (a)-$G(3) \leftarrow B(7)$ and $\leftarrow B(7)$ bands obtained from a ClF (3 Torr) – Xe (10 Torr) + He (50 Torr) mixture. The pump laser was tuned to the $B(7,20) \leftarrow X(0,19)$ transition. Note the enhanced intensity for the $J = 10$-19 levels due to the heterogeneous multilevel $B^3\Pi_0$-~$A^3\Pi_1$ perturbation centered at $J = 14$. Transitions from both components of the $B(7,14)$ level are shown in the P branch by the dashed lines. [Reproduced by permission from the *Journal of Chemical Physics*.].

principal concern,[4] since the irregularities due to the homogeneous interaction between β and G states are much larger than the experimental uncertainties, ~1 cm^{-1}, in vibrational energy and 1% for B_v. Clearly, the observed vibrational energies and rotational constants cannot be fitted by standard power series expansions. Unlike the Ω–0^+ states, the rotational constants for the lower vibrational levels of the Ω –1 states with close absolute energies did display systematic differences (Figure 5b), which enabled assignment of a given vibrational level to either the β or G state with some confidence.[4]

For a few low levels of β, in particular v' – 0-2 and 4, a more extended rotational structure was observed (Figure 9b). This result is due to the heterogeneous interaction between the β and E states, which mixes the e-components of Ω –0$^+$ and Ω –1 basis functions allowing $\Delta\Omega$ –1 transitions with the same selection rules as the parallel $\Delta\Omega$ –0 transitions. This type of perturbation has been thoroughly documented for other ion-pair states of halogens.[22,27,28] According to the theory, the heterogeneously interacting states must have a common dissociation asymptote. In particular, the G and E states do not interact. The interaction between E and β splits the doubly degenerate e- and f-sublevels of the β state (the effect often is called Ω doubling). In OODR experiments with pumping through the $B(^3\Pi_{0^+})$ state, only e-sublevels of the ion-pair states were accessed. However, both e- and f-subcomponents of β, v –0 were observed and assigned in the high resolution emission spectrum of ClF excited by the Tesla coil discharge.[7] The difference in rotational constants for the e- and f-sublevels of β, v' –0 was quite large, $B_v(f)$–$B_v(e)$–0.0067 cm^{-1}; see Figure 5b. This strong heterogeneous interaction explains the "strange" increase in B_v for v'–0-2 of the β state (e-type levels) observed in the OODR results of Figure 5b, i.e., the heterogeneous interaction becomes smaller as v' increases. This heterogeneous interaction also is partly responsible for the larger than expected B_v values for low levels of the $E(0^+)$ state. As shown for Br_2 and Cl_2, both subcomponents of the β state can be accessed by OODR, if the pumping is through $A(^3\Pi_1)$ as the intermediate state.[23]

To confirm the original vibrational level assignment for the β and G states[4] and to search for strongly perturbed pairs of levels, measurements of isotopic shifts for the β and G levels have been carried out. Most experiments were performed with the pump laser tuned to the ^{35}ClF(B(7,14) ← X(0,15)) and ^{37}ClF(B(7,17) ← X(0,16)) spectrally overlapped transitions. Fortunately, the ^{35}ClF(B(7,14)) and ^{37}ClF (B(7,17)) levels are perturbed by the A state (see Table 1) and transitions to the Ω –1 ion-pair states can be easily observed for both isotopomers. A typical OODR excitation spectrum to $f(v'$–11) and $G(v'$–16) is shown in Figure 10 as an example. Measurements for ^{35}ClF were extended up to the v'–18 and 14 levels for the β and G states, respectively. Although the spacings between the v'–0-4 levels of G are much larger than for β, the situation is reversed for v'–6-11 and above v'–11 the spacings are similar. The isotopic shifts are plotted *vs.* total energy of the β and G vibrational levels

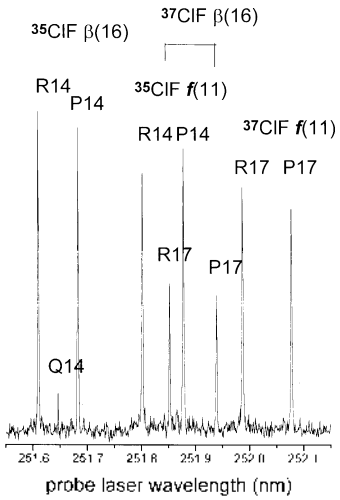

Figure 10. Excitation spectrum of the $f(11) \leftarrow B(7)$ and $\beta(16) \leftarrow B(7)$ bands of ^{35}ClF and ^{37}ClF. The pump laser was tuned to the ^{35}ClF(B(7,14) ← X(0,15)) and ^{37}ClF(B(7,17) ← X(0,16)) spectrally overlapped transitions in 1 Torr of ClF.

in Figure 7b. The isotopic shifts for the v'–4-10 levels of the G state and for the v'–8-13 levels of the β state show irregularities that suggest strong homogeneous interactions over this whole energy range. These same interactions probably are partly responsible for the switch in the energy level spacings mentioned above. These stronger and more extensive interactions, relative to the E and f states, may be due to the closeness of the inner branches of the β and G potentials, which could result in large Frank-Condon overlap integrals. The *ab initio* calculations[8] also predict that the repulsive branches of the G and β potential curves are closer together than the E and f branches.

The $D'(\Omega = 2)$ and $\Omega = 0^-$ ion-pair states. Direct transitions by OODR experiments to the D' state are forbidden from B or from mixed B~A levels due to the $\Delta\Omega$ –0 selection rule. But to our surprise, we were able to observe the $D'(2)$ state in OODR experiments *via* pumping through the B(9,10) perturbed level.[6] This result suggests that this perturbed level must have an admixture of Ω –2 basis function from the $A'(^3\Pi_2)$ valence state or from yet another Ω –2 state (presumably weakly bound) that also correlates to Cl ($^2P_{3/2}$) + F($^2P_{3/2}$). The B(9,10) level is just ~100 cm^{-1} below this dissociation limit and the density of levels is high. Since direct interaction of the $B(\Omega$ –$0^+)$ and $A'(\Omega$ –2) states is forbidden, presumably an accidental three-state perturbation B~A~A' takes place resulting in a mixing of the Ω –0^+, 1, and 2 basis functions. Remarkably, such an accidental B~A~A' three-state perturbation was also observed in Cl_2.[21b] In our searches, the only rotational state of $B(^3\Pi_{0^-})$ that showed this behavior, *i.e.*, access to the D' ion-pair state, was J – 10 of v – 10. These excitation spectra, plus the experiment below for v'–2, gave vibrational energies (±1 cm^{-1}) and rotational constants (±1%) for 11 vibrational levels. An interesting aspect of the spectra shown in Figure 11 is the presence of Q branches, which are expected[20c] for excitation from $A(^3\Pi_1)$ to $\beta(1)$ or $G(1)$ states for low J. The presence of

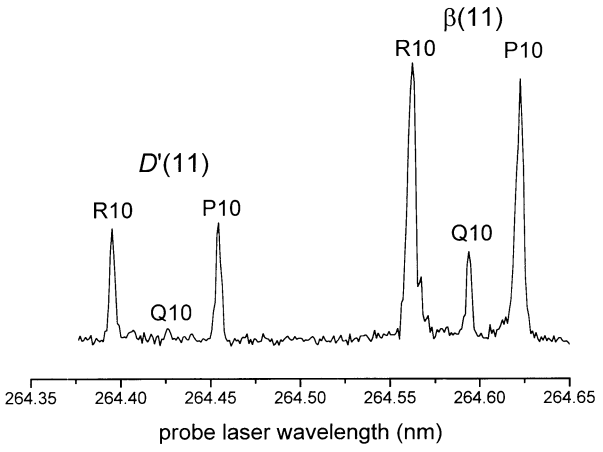

Figure 11. Excitation spectrum showing transitions to the $D'(11)$ and $\beta(11)$ bands obtained by pumping the perturbed $B(9,10)$ level at a ClF pressure of 0.7 Torr. A similar spectrum for $D'(3)$ and $\beta(3)$ is shown in reference 6.

the Q branch suggests a relatively strong admixture of Λ character into the $B(v-10, J-10)$ level. The D', $v'-2$ level was an exception to all the other v' levels, and despite several attempts it could not be excited using the $J-10$ level of $B(v-10)$. However, transitions from *unperturbed* high J levels of $B(7)$ to D', $v'-2$ were observed in OODR experiments (Figure 12). The effect is strongly J dependent and only transitions from the $J>20$ levels could be observed. An explanation is that an admixture of $\Omega=0^-$ basis function to D', $v'-2$ must exist, arising from heterogeneous interaction with β, $v'-2$ which, in turn, is perturbed by $E(v'-2)$. In other words, the heterogeneous interaction of D' with E is mediated through $\beta(v'-2)$. Since D', $v'-2$ was not observed from pumping the $B(7,15)\sim A(9,15)$ mixed level, the $\beta\sim D'$ mixing must dramatically increases with J. This upper state heterogeneous interaction between D' and E was not observed for any other D' vibrational level. The $E\sim\beta\sim D'$ heterogeneous mixing has been observed in other halogen molecules too.[27b] Due to the similarity of the ion-pair state potentials, the three-state mixing can take place for several consecutive vibrational levels, as long as the levels in the three states separate slowly because of slight differences in vibrational constants. In contrast, the $E\sim\beta\sim D'$ heterogeneous mixing for

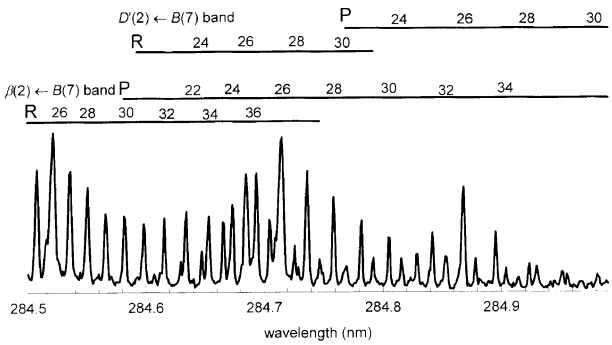

Figure 12. Laser excitation spectra of $\beta(2) \leftarrow B(7)$ and $D'(2) \leftarrow B(7)$ bands obtained with the pump laser tuned to the $B(7,26)$ level. The ClF pressure was 5 Torr.

ClF occurs rather accidentally; the homogeneous interaction of E with f and β with G accidentally shifts the $v'-2$ levels of the three E, β, D ion-pair states (see Figure 4) into close proximity.

Unlike the $\Omega=0^-$ and $\Omega=1$ states, the $D'(\Omega=2)$ state is not perturbed homogeneously, and its vibrational levels can be fitted by standard Dunham series expansions.[6] The energies of the vibrational levels and the rotational constants that were deduced from a single P-R doublet from the laser excitation spectra were combined with the high resolution results for $v'=0$ and 1 from analysis of the D'-A' emission bands excited by a Tesla coil discharge, and the constants for the D' state are presented in Table 3. With these constants, the vibrational energies can be calculated to ± 1 cm^{-1} uncertainty through $v'=16$. The D', $v'=0$ level lies 158 cm^{-1} below the next state β, $v'=0$.

Considering the expected similarity of ion-pair potentials, all the ion-pair states of Cl$^+$F$^-$ would have spectroscopic constants similar to those of D', if the homogeneous interactions between $\beta(1)$-$G(1)$ and $E(0^-)$-$f(0^-)$ were negligible. Comparison of these five ion-pair potentials of ClF with those of Cl_2 is of interest. Ishiwata and coworkers[20,21] found that all six gerade ion-pair states of Cl_2 had regular potentials with very similar spectroscopic constants, ω_e=252-257 cm^{-1}, $\omega_e x_e$=1.02-1.20 cm^{-1} and R_e=2.87-2.90 Å, which implies a negligible degree of interaction between the $^3\Sigma_{0_g^+,1_g}$ and $^3\Sigma_{0_g^-,1_g}$ ion-pair states. The $^3\Sigma_g^+$ and $^3\Sigma_g^-$ states arise from MO configurations that differ by permutation of two electrons, $(\sigma_g)^2(\pi_u)^2(\pi_g)^4(\sigma_u)^2$ and $(\sigma_g)^1(\pi_u)^4(\pi_g)^3(\sigma_u)^2$, respectively, which presumably is part of the explanation for the absence of interactions. In contrast, the $^3\Sigma^-_{0_u^-,1_u}$ and $^3\Pi_u$ states of Cl_2 differ by one electron permutation in their leading MO configuration, $(\sigma_g)^2(\sigma_u)^2(\pi_g)^3(\pi_u)^2$ and $(\sigma_g)^1(\sigma_u)^2(\pi_g)^4(\sigma_u)^2$, respectively, and the 1_u and 0_u^- pairs were found to interact.[29] As for ClF, the upper ungerade potentials have a larger value of ω_e than the lower states, 284 *vs* ~235 cm^{-1}. The homogeneously unperturbed ungerade ion-pair states of Cl_2, $^3\Pi_{0_u^+}$ have ω_e – 248 cm^{-1}. The differences between the 1_u and 0_u^- pairs, as well as their differences from the unperturbed states, cannot be ascribed to intrinsic properties of these states, and they must be a result of homogeneous interactions.

With 5 of the ion-pair states from the Cl$^+$($^3P_{J=0,1,2}$) + F($^1S_0$) cluster being assigned, the 0^- state is the only one remaining unknown. Access to this state is forbidden by the $0^- \leftarrow|\rightarrow 0^-$ rigorous selection rule. Ishiwata and coworkers were able to detect the $0_{g,u}$ ion-pair states of Cl_2 in OODR experiments by pumping through the mixed $A^3\Pi_{1_u}\sim 1^3\Pi_0$- rovibronic levels.[12,29c] Unfortunately, the weakness of the $A \leftarrow X$ transition in ClF prevented a search for similar perturbations. In principle, heterogeneous mixing of the $G(1)$ and 0^- upper states, similar to that found between the $\beta(1)$ and $E(0^-)$ states, is yet another possible way to access the 0^- state. However, we did not find any evidence of $G(1)\sim 0^-$ mixing using the perturbed $B\sim A$ levels as intermediates in OODR experiments.

Although the 0^- state was not observed experimentally, its

Table 2. Energy (cm^{-1}) separation of the v'=0 Levels of the Ion-Pair States Arising from $Cl^+(^3P_J)+F^-(^1S)$[a,b]

Cl^+F^- state	calc.[c]	calc.[d]	experimental
D'	0	0	0
β	157	151	161
E	254	240	237
0^-	659	684	
G	959	955	972
f	1193	1210	1185

[a]Relative to D', v' 0. [b]Formulas for the energies of the $Cl^+(^3P_J)$ + $F^-(^1S)$ multiplet were taken from Ref. 30 and 20e. [c]ζ = 648.6 cm^{-1} and Π-Σ = 457.4 cm^{-1}: ζ and Π-Σ were treated as variable parameters in this calculation. [d]ζ = 684 cm^{-1} and Π-Σ = 422.5 cm^{-1}: Π-Σ was a variable parameter, the ζ value was taken as the same as for the ion-pair states of Cl_2 (Ref. 20e).

potential should be very similar to that of D'. The location of 0 state can be estimated using the method developed by Cohen and Schneider[30] and adapted for the halogen ion-pair states by Ishiwata and coworkers.[20e] According to Cohen and Schneider, the spin-orbital splitting of states arising from ^3P_J + ^1S separated atom limit can be rationalized with just three parameters: ζ- the spin-orbit constant of the ^3P atom, Σ- the destabilization energy due to overlap of the p_σ orbital of the ^3P atom with the filled p_σ orbital of the ^1S atom and Π- the destabilization energy due to overlap between the p_π orbital of ^3P atom and the filled p_π orbital of the ^1S atom. Values for Σ and Π can be calculated from energies of the experimentally observed ion-pair states (in fact, Σ and Π are not independent parameters and only their difference can be deduced from calculations). Ishiwata and co-workers[20c,29a] applied this approach to the gerade and ungerade ion-pair states of Cl_2 and found that the experimental and calculated energies were within ± 30 cm^{-1}. For ClF the agreement is even better (Table 2). The predicted splitting between the D' and 0 states is very close to the spin-orbit constant for Cl^+, ζ –697 cm^{-1}. This finding has been confirmed for Cl_2 by experiment, $T_e(0_g)$-$T_e(2_g)$–683 cm^{-1} and $T_e(0_u)$-$T_e(2_u)$–670 cm^{-1}. The *estimated* positions of the unperturbed energy levels of the 0 state are shown on the right hand side of Figure 4.

The good agreement between the calculated and experimental energy differences for the T_e and T_0 values of the homogeneously perturbed Ω –1 and Ω –0$^-$ pairs, implies that the shifts of v'–0 levels from their unperturbed positions are less than 20 cm^{-1}. This result is somewhat surprising considering the big difference (~100 cm^{-1}) in the vibrational quanta of the $E(0^+)$ and $\beta(1)$ *vs.* the $f(0^-)$ and $G(1)$ states (Figure 4). Apparently, the interaction distorts the ion-pair potentials, but leaves the T_0 values almost intact.

In addition to comparing the spin-orbit splitting of the ClF and Cl_2 states, the respective bond dissociation energies and R_e values of the unperturbed D' (Ω –2) states are of interest. The dissociation energies (D_e values) are 43,820 and 38,800 cm^{-1} for ClF[6] and Cl_2,[21b] respectively. The smaller bond energy of Cl_2 correlates with its larger internuclear distance 2.874[26b] *vs.* 2.507[6] Å for ClF. These differences in bond lengths are consistent with the ionic radii of F$^-$ *vs.* Cl$^+$.

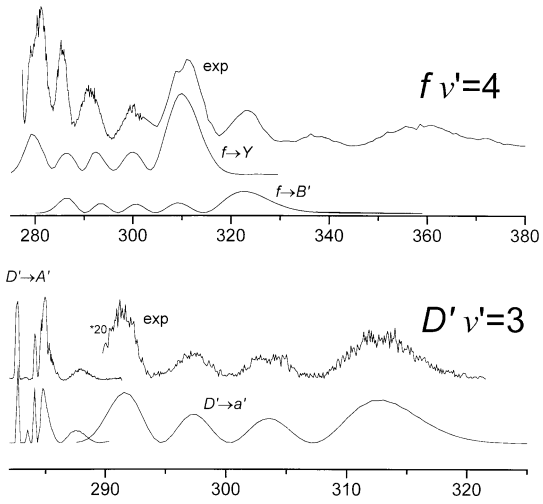

Figure 13. Comparison of the experimental and calculated bound-free emission spectra from the $f(0^+)$, v' 4 and $D'(2)$, v' 3 levels. The intense emissions for the < 290 nm range is the $f \rightarrow B$ transition in the upper panel and the $D' \rightarrow A'$ transition for the lower panel. The calculated spectra for the $f \rightarrow Y$ and $f \rightarrow B'$ transitions should be coadded for comparison to the experimental spectrum.

The repulsive Ω =0$^+$, 1 and 2 valence states of ClF. A typical OODR emission spectrum from a given v' level of an ion-pair state displays bound-bound transitions to one of the weakly bound valence states plus broad, structured, bound-free spectra to other repulsive valence states toward longer wavelengths. Two experimental spectra are compared with the computed spectra in Figure 13 from the $f(0^-)$, v' –4 and $D'(2)$, v' –3 levels. We undertook a systematic experimental survey of the bound-free emission spectra from the $v' < 9$ vibrational levels of the ion-pair states in order to deduce repulsive valence state potentials and transition dipole functions from computer simulation of the bound-free spectra.[5,9] A better understanding of the repulsive valence states is the only area where the spectroscopy of ClF is somewhat ahead of that for Cl_2.

Fitting the bound-free emission spectra from the D' state was straightforward. The potential for the D' state could be accurately represented by a Rittner potential[6]; only four Ω –2 valence states exist and one of them, $A'(^3\Pi_2)$, is the well characterized bound state. The remaining three states are repulsive with dominant MO configurations 2341($^3\Pi$ or $a'^3\Pi_2$) and 2422($^1\Delta$ and $^3\Delta$). According to the theory, only the allowed transition to the 2341 ($a'^3\Pi_2$) state should have significant intensity. This predicted result was confirmed by the experiment,[9] (see Figure 13) and all the bound-free spectra from the D' state could be fitted by a transition to one lower state. The analytical expression for the $a'^3\Pi_2$ potential deduced from fitting the experimental spectra from several D' vibrational levels is given in Table 3, and a plot of the potential for $R \geq 2.2$ Å is shown in Figure 1.

Three repulsive Ω –0$^-$ valence states (Table 3) exist and transitions to all of these states were observed in emission spectra from the Ω –0$^-$ ion-pair states.[5] Computer simulation of the bound-free spectra to deduce analytical expressions

Table 3. Repulsive valence state potentials of ClF

Dissociation limit $Cl(^2P_J)+F(^2P_J)$	L-S coupling	MO configurations and their weight[a,b]		Analytical formula for potential (R in Å units)[c]
		2332	0.816	
3/2 + 3/2	$1^3\Sigma_{0+}$	2422	0.083	$3.814\times10^6 R^{-7} - 1.02\times10^5 R^{-5} - 7.4\times10^6 R^{-9} + 2.15\times04$
		2341	0.676	
3/2 +1/2	$B'^3\Pi_{0+}$	1342	0.154	$1.8\times10^6 R^{-11} + 2.01\times10^6 R^{-7} - 6.56\times10^4 R^{-4} + 2.24\times10^4$
		1432	0.071	
		2332	0.839	
1/2 +1/2	$C^1\Sigma^+_{0+}$	2422	0.054	$2.51\times10^6 R^{-9} + 2.05\times10^6 R^{-7} + 2.28\times10^4$
3/2 + 3/2	$^3\Pi_1$	?		$3.55\times10^6 R^{-8} - 1.76\times10^5 R^{-6} + 2.15\times10^4$
3/2 + 1/2	$^3\Sigma^-_1$	?		$2.36\times10^6 R^{-7} - 8.7\times0^3 R^{-2} + 2.19\times10^4$
1/2 + 3/2	$^3\Sigma^-_1$ or $^3\Delta_1$	?		
				$2.2\times10^6 R^{-7} + 2.24\times10^4$
3/2 + 3/2	$a'^3\Pi_2$	2341 (dominant)		$1.45\times10^7 R^{-10} + 2.15\times10^4$

[a]The configuration $\sigma^k\pi^l\pi^{*m}\sigma^{*n}$ is abbreviated to *k l m n*. [b]Configurations were obtained from calculations at R = 2.43 Å, but the reader should consult ref. 8 and 9 for more complete information. [c]Taken from Refs. 5, 8 and 9.

for the repulsive potentials was not so straightforward as for the D' state case for several reasons. The potentials for the E and f states were approximated by Morse functions with vibrational parameters based on average values of ω_e and $\omega_e x_e$ for the first ten vibrational levels. Computer simulation of the bound free spectra from the $E(0^+)$ state gave satisfactory results based upon transitions to $Y(^3\Sigma^-_0)$ and $^3\Sigma_{0^+}$ for v'=0-6. The bound-free spectra from the f, v'=0, 1 and 2 levels also could be fitted by transitions to the same B' and Y repulsive potentials. The bound-free spectra from the f, v'=3 and E, v'=7 strongly interacting levels (see the isotopic shifts of Figure 7) could not be interpreted by treating either level separately. An attempt to calculate spectra from the mixed vibrational wavefunctions for these perturbed levels was partly successful (see Ref. 5 for more details). The $Y(0^+)$ state crosses the $B(^3\Pi_{0^+})$ potential and it is responsible for predissociation of the latter.

The bound-free spectra from the f, $v' \geq 4$ levels clearly showed transition to the Y and B' potentials. However, another series of long wavelength bands still remained unassigned (see Figure 13). In the original interpretation,[5] these bands were assigned as transitions to a third state, $C(0^+)$, and a repulsive potential was developed for that state. It should be noted that these experiments were conducted at pressures of ~1 Torr of ClF and no evidence exists for collisional transfer between vibrational levels of the initially excited state or transfer to vibrational levels of other ion-pair states. Such transfer events would have been readily detected in the spectra of the more intense wavelength resolved bound-bound transitions.

Comparison of the experimentally assigned repulsive potentials and dipole moment functions for the bound-free transitions with results from the *ab initio* calculations are discussed in Ref. 8. The level of agreement is generally quite satisfactory for the range of R sampled; however, one question remains unanswered. As noted above, the spectra from the f, $v' \geq 4$ levels showed weak, broad oscillating emission at longer wavelength than the $f \rightarrow Y$ and $f \rightarrow B'$ transitions. The *ab initio* calculations gave a small $f \rightarrow C$ transition dipole, and the authors question the assignment of this emission to transitions terminating on the C state. Another possible explanation for these bands (which are not strong features of the spectra) is mixing of the $f(v > 4)$ levels with E state vibrational levels; the latter do have transitions to longer wavelength because a smaller range of internuclear distance is sampled by vibrational motion in the E state potential. The arguments would be formulated in the same way as for the E, v' =7 and f, v' =3 pair, but the degree of mixing presumably is less. Since the Morse potentials used to represent the f and E states are not exact, several variables must be considered in an interative fashion to further refine the fitting of these overlapping bound-free emission spectra.

Simulation of the bound-free spectra from the Ω =1 ion-pair states has proven to be the most complex of the three cases, and the work is still in progress.[9] In addition to the necessity of defining effective β and G potentials, eight Ω =1 valence states exist and only one of them, $A(^3\Pi_1)$, is bound. The upper states are nominally triplet states, so only triplet valence states were considered as lower states. The *ab initio* calculations predicted that transition to two out of the seven repulsive states should have negligible intensity.[9] Thus, transitions to five states are to be considered when fitting the bound-free spectra from G and β states. Further complications may arise because of the homogeneous perturbation between certain pairs of vibrational levels in β and G; see Figure 7. All of these questions will be discussed in a separate report.[9] At the present time, three of the Ω =1 potentials have been qualitatively fitted and those potentials are listed in Table 3. One interesting point is that the problem mentioned above for fitting the long wavelength spectra for the f, $v' \geq 3$ levels also exists for the spectra from the G, $v' \geq 3$ levels. According to the isotopic shift data, this is the range where the β and G vibrational levels are expected to be strongly mixed.

The $^3\Pi_{0^+,1,2}$ valence states of ClF. The $B(^3\Pi_{0^+})$ state has been known since 1968.[24] McDermid[25] significantly improved our understanding of the spectroscopy, including identification of perturbed levels, using laser-induced fluorescence in

Table 4. Spectroscopic Constants (cm^{-1}) for the A', A and B Valence States of $^{35}Cl^{19}F$[a]

	$A'^3\Pi_2$	$A^3\Pi_1$	$B^3\Pi_{0^+}$
T_e	18257	18512	18825
D_e[b]	3243	2988	3079
ω_e	363.5	361.2	362.6
$\omega_e x_e$	-8.3	-7.7	-8.2
B_e	0.3341	0.3341	0.3349
α_e	-0.0063	-0.00638	-0.0074
R_e(Å)	2.0245	2.0247	2.0221

[a]More complete sets of constants can be found in Refs. 6 and 7. [b]The A' and A states dissociate to two ground state atoms, which lie 21500(2) cm^{-1} above the minimum of the X state; the B state dissociates to Cl($^2P_{3/2}$) + F($^2P_{1/2}$), which lies 404 cm^{-1} higher.

1981. Tellinghuisen[6,7] combined several sources of spectroscopic data to improve and develop potentials for the $B(^3\Pi_{0^+})$, $A(^3\Pi_1)$ and $A'(^3\Pi_2)$ valence states. The B state was reanalyzed with use of published data from Ref. 24 and 25 plus our OODR spectra for E and $f \leftarrow B$ transitions with extensive rotational structure. In addition, the 0-6 band of the $E \rightarrow B$ transition, was recorded at high resolution from the Tesla discharge. Simultaneous fitting of all these data gave more accurate constants for the B state (Table 4). The B state dissociates to F($^2P_{1/2}$) and Cl($^2P_{3/2}$) and the potential is experimentally characterized to within a few cm^{-1} of the dissociation limit. As with other interhalogen molecules, the $B^3\Pi_{0^+}$ potential is crossed by the repulsive $Y(0^-)$ potential that correlates to the $^2P_{3/2} \cdot {}^2P_{3/2}$ limit and causes predissociation. This predissociation for ClF(B), which occurs at $v = 9$, $J \geq 21$ and $v = 10$, $J \geq 13$, is relatively weak and levels above $v = 10$ can be observed in adsorption[24] and in emission[4] from the E or f states.

The A' state was characterized[6] by analysis of high resolution data from the $D' \rightarrow A'$ emission spectrum excited by a Tesla coil discharge. A total of ~1000 lines in 9 bands were assigned, these bands are $v'=0 \rightarrow v'' = 4, 5, 6, 7$ and $v'=1 \rightarrow v'' = 3, 4, 5, 7, 8$ for ^{35}ClF and one band, $v'=0 \rightarrow v'' = 5$, for ^{37}ClF. A low resolution emission spectrum from $D'(v'=5, J'=10)$ obtained in an OODR experiment displayed transitions to the v''=8-14 levels, and these data were used to extrapolate the A' state potential to near the dissociation limit with an accuracy of ~5 cm^{-1} for vibrational energies and ~0.01 cm^{-1} for the rotational constants of all vibrational levels above v=8.

The A state potential was characterized[7] using rather sparse data taken from several sources: (i) direct observation of a few levels of the $A \rightarrow X$ transition using the UV labeling technique (see below) in OODR experiments, (ii) direct observation of the 0-4 band of the $\beta \rightarrow A$ spectra in Tesla coil discharge spectrum, (iii) identification of $A'(6)$~$A(5)$, $B(6)$~$A(8)$ and $B(7)$~$A(9)$ perturbations (see Table 1). Those data provided accurate spectroscopic constants for $v = 4, 5, 8$, and 9 levels of the $A(^3\Pi_1)$ potential. Considering the similarity of all three $^3\Pi$ valence potentials of ClF and properties of the A state potentials in other halogens, reasonably reliable spectroscopic constants for ClF(A) were obtained and these are given in Table 4.

The OODR experiments employing the UV labeling technique deserve a separate note. The probe laser was tuned to a known $Cl^1F \leftarrow ClF$ (B; v, J) resonance and fluorescence from the Cl^1F state was observed. The pump laser was scanned over vibrational-rotational levels of the B state, and all rovibronic levels that are collisionally coupled with the probed Cl^1F level can be observed as a $B \leftarrow X$ excitation spectrum. Such experiments[7] provided excellent spectra for the $v = 7$ and 8 levels of the B state for a ClF pressure of 7-8 Torr. We tried to use this technique to find weak $A \leftarrow X$ transitions. However, only $B \leftarrow X$ lines were observed in the spectrum when the probe laser was tuned to the $E, f \leftarrow B$ or even the $\beta \leftarrow B$ rovibronic transitions (Figure 14). The whole situation changed dramatically, however, when the probe laser was tuned to the resonance from the $B(7,14)$~$A(9,14)$ mixed level to the β, $v' = 2$ and G, $v' = 2$ levels. The excitation spectrum revealed rotational lines for the previously unknown $A^3\Pi_1$ state as an $A(9) \leftarrow X(0)$ transition, see Figure 14. These observations suggest that the B and A electronic states are not easily coupled by collisions with ClF, and only the mixed levels provide doorways from one electronic state to another. Supporting evidence for this view is the general absence of β or $G \leftarrow A(^3\Pi_1)$ transitions in experiments where the probe laser was scanned following pumping of $B(^3\Pi_{0^+})$ levels in the presence of high pressures of He, e.g., see Figure 3. Collision coupling between the A and A' states might be more effective, since those states correlate to the same atomic dissociation limit. Collision-induced predissociation in the B states of several halogen molecules has been extensively studied.[2,31-35] Although the collision transfer rates among the A', A and B states of the halogens seem to be rather slow, additional state-selected experiments are needed for documentation.

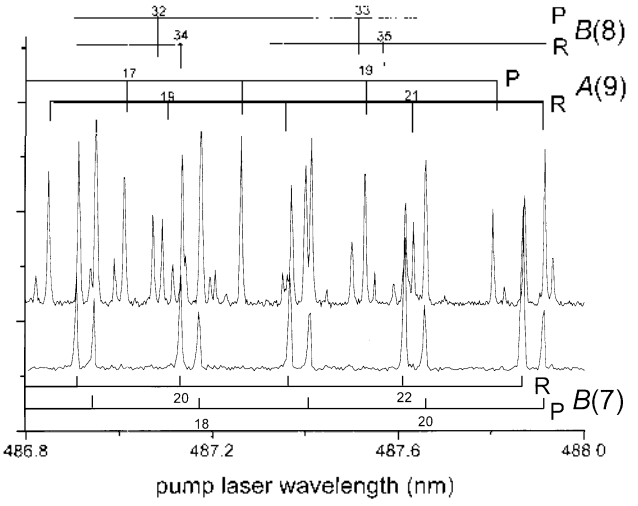

Figure 14. Segment of the laser excitation spectra obtained by scanning the pump laser in the range of $B(7) \leftarrow X(0)$ transition with the probe laser tuned to the P(24) line of $\beta(2) \leftarrow B(7)$ band (lower spectrum) and to the overlapping $R(14)$ (^{35}ClF) and $R(17)$(^{37}ClF) lines of the $G(2) \leftarrow B(7)$ band (upper spectrum). The latter shows direct transitions to $A(9)$ as well as $B(8)$. The ClF pressure was ~10 Torr.

The similarity in molecular properties of Cl_2 and ClF give a reason to expect that the $1(^3\Pi_{0^-})$ state of ClF will be bound. Ishiwata and coworkers[12] observed this state of Cl_2 by exciting the 0_g^- ion-pair state through mixed $A(^3\Pi_{1u})$–$1(^3\Pi_{0_u^-})$ levels and observing the dispersed $0_g^- \rightarrow 1(^3\Pi_{0_u^-})$ emission spectra. As already noted, the weakness of the $A \leftarrow X$ transition is a major obstacle for a systematic search of similar perturbations in ClF. The $1(^3\Pi_{0_u^-})$ state of Cl_2 is ~612 cm^{-1} above the A' state[12,26a] and a similar splitting may be expected between those states for ClF. In this context, comparing the positions of the A and B states relative to A' is worthwhile. The values in cm^{-1} are 282(255) and 539(568) for the A and B states for Cl_2(ClF). The bond dissociation energy (D_e) values of the $A'(^3\Pi_0)$ states also are quite similar (3110[26a] *vs.* 3243 cm^{-1}) with ClF being 133 cm^{-1} larger. The difference in D_0 values is only 80 cm^{-1}. These similarities exist even though the bond length of Cl_2(2.43 Å) is considerably larger than for ClF(2.02 Å) for these states.

The radiative lifetimes of the B states of ClF and Cl_2 also are similar, 0.35 and 0.30 ms, respectively.[2,36] Since the absorption to the ClF($A^3\Pi_1$) state seems more difficult to observe than for Cl_2, the lifetime for the $A(^3\Pi_1)$ state of ClF may be longer than for Cl_2, but both probably are longer than 1 ms. Now that the ClF($A^3\Pi_1$) levels have been characterized,[7] further searches for direct absorption using the OODR technique with a more powerful pump laser and higher ClF pressures might be worthwhile. Since individual vibrational levels of the valence states now can be monitored by laser-induced transitions to the ion-pair states, the opportunity exists for detailed kinetic studies of relaxation among the bound valence states. The OODR method would circumvent the difficulty of trying to use the weak fluorescence from the long-lived $B(^3\Pi_{0^+})$ and $A(^3\Pi_1)$ states[2,31-34] to monitor the kinetic processes.

The ground state of ClF. The ground state potential has been characterized with respect to vibrational energy up to $v=9$ from $B \rightarrow X$ chemiluminescent spectra.[37] These data were combined with high resolution absorption data[24] for $v=0$ and 1 to obtain vibrational constants. The rotational constants seem to be derived from the high resolution data and microwave measurements for a few low vibrational levels. We did observe emission bands to high vibrational levels (v = 27-34) of the ground state in some of the OODR experiments in which low levels of the $I(0^+)$ ion-pair state were excited.[39] Systematic experiments of this nature with higher resolution could be used to better define high vibrational levels in the $X(^1\Sigma^+)$ potential.

The conventional gas phase absorption spectrum of Cl_2 and ClF consists of very weak bands arising from transitions to the Franck-Condon favored levels of $B(^3\Pi_{0^+})$ in the 500 nm range followed by much stronger absorption to the repulsive valence states at shorter wavelength. The dominant transition for Cl_2 is to the $1(^1\Pi)$ potential with a maximum at 330 nm.[1] The maximum in the corresponding absorption spectrum for ClF is at 260 nm and the extinction coefficient for ClF seems to be about a factor of 3 smaller.[38] Assuming that transitions to the $1(^1\Pi_1)$ potential dominates the absorption spectrum of ClF, this potential must be somewhat more repulsive than for Cl_2, which could be expected since $R_e(ClF(X)) < R_e(Cl_2(X))$. Visual inspection of $ClF(1^1\Pi_1)$ potential from the *ab initio* calculations[8] suggest an absorption maximum near 270 nm, which may prove to be in close agreement with the experimental spectrum after account is made for the thermal population in the ground state. The experimental bound-free emission spectra mentioned in this report terminate on triplet lower repulsive states. However, OODR excitation of the $\Omega=1$ ion-pair state that correlates to $Cl^-(^1D_2)F^-$ could provide bound-free emission spectra that would sample the $^1\Pi_1$ potential for $R \geq 2.3$ Å. Such work would more completely define the $1(^1\Pi_1)$ potential and further our understanding of the ultraviolet absorption spectrum of ClF.

Summary

Five ion-pair states, two bound valence states and 7 repulsive valence states of ClF have been experimentally characterized using mainly the OODR technique. The measurements include both ^{35}ClF and ^{37}ClF isotopomers. Several of the OODR experiments were achieved only because of perturbations among vibrational-rotational levels of the $B(^3\Pi_{0^+})$ and $A(^3\Pi_1)$ valence states, which are interesting subjects in their own right. The most intriguing question about the electronic states of ClF that have been investigated so far is the explanation of the irregular vibrational energies of the $I(0^+)$ and $f(0^+)$ pair and the $\beta(1)$ and $G(1)$ pair. Fortunately, the vibrational levels of the D' state are regular and unperturbed and they provide a valuable reference. The *ab initio* calculations[8] with spin-orbit coupling suggest a partial resolution of this dilemma. The diabatic $^3\Pi$ and $^3\Sigma^-$ ion-pair potentials arising from $Cl(^2P_J) + F^-(^1S_0)$ actually cross near the minimum of the $^3\Sigma^-$ potential, *e.g.*, the $^3\Pi$ potential is more repulsive and crosses the $^3\Sigma^-$ potential from below. After the spin-orbit coupling is included (case c coupling), adiabatic potentials are obtained for $I(0^+)$ and $f(0^+)$ together with $\beta(1)$ and $G(1)$. According to the calculations, these potentials change their nature near their minimum, e.g., the $I(0^+)$ potential has $^3\Pi_{0^+}$ character for $R \geq 3.4$ Å and $^3\Sigma_{0^+}^-$ character for $R \leq 3.4$ Å. The $f(0^+)$ state has just the opposite nature. This diabatic curve crossing does rationalize the higher (on average) ω_e values for the $f(0^+)$ and $G(1)$ states relative to $I(0^+)$ and $\beta(1)$. The resulting adiabatic potentials have some distortion near the bottoms of the potentials, and this distortion can partly explain the irregular vibrational energy spacings of the low levels. However, the irregular spacings extend to high v' levels where the calculated potentials are quite smooth. Thus, pairwise interactions must exist between certain vibrational levels in the $I(0^+)$ and $f(0^+)$ states or the $\beta(1)$ and $G(1)$ states, as the ^{37}ClF isotopomer data presented here more fully documents. In some cases, these interactions may extend beyond pairwise interactions and include several vibrational levels.[39] Since the calculated crossing distance for the diabatic potentials may not be exactly correct, separating these various effects is going to

be very difficult, and it is a subject requiring additional work.[9,39] These factors also affect the rotational constants of the vibrational levels of the $E(0^+)$, $f(0^+)$, $\beta(1)$ and $G(1)$ states. In addition, the rotational constants of some of these levels also are affected by heterogeneous perturbations, and the variation of the rotational constants of these states with vibrational energy is quite complex. Additional experiments in which the *e*- and *f*-components of more vibrational levels of the $G(1)$, $\beta(1)$ and $D'(2)$ states are characterized would provide useful data to help clarify the interactions.

The abrupt change in molecular character of the $E(0^+)$ and $f(0^+)$ or $\beta(1)$ and $G(1)$ near the minima of their potentials has several implications. The transition dipole function for the $E(0^+) \rightarrow B(^3\Pi_{0^+})$ transition of Cl_2 has been obtained from analysis of experimental intensity data.[40] The function declines monotonically for $R \geq 2.6$ Å, as generally is expected for a charge-transfer type transition. In contrast, the calculated $E(0^+) \rightarrow B(^3\Pi_{0^+})$ transition-dipole function for ClF goes through a pronounced maximum at ~R_e(2.5 Å) and declines for both smaller and larger R. The maximum in the function clearly is associated with the crossing of the $^3\Pi_{0^+}$ and $\Sigma^-_{0^+}$ potentials. In fact, the ion-pair states of Cl_2 derived from the $^3\Pi_g$ configuration have lifetimes of 4-5 ns, whereas those derived from $^3\Sigma_g^-$ have lifetimes of 45 ns[41] and the transition dipole functions of the adiabatic states of ClF should reflect the crossing distance of the diabatic potentials. Careful measurement of the relative emission intensities for all transitions from a range of $E(0^+)$ and $f(0^+)$ vibrational levels would be useful. Measurement of the radiative lifetimes of $E(0^+)$ and $f(0^+)$ plus those for $\beta(1)$ and $G(1)$ also could be helpful for better definition of the $^3\Pi$ and $^3\Sigma^-$ character of the adiabatic states, as well as elucidating the secondary homogeneous perturbations between specific vibrational levels.

Finding the ion-pair and bound valence states with 0^- symmetry remains as a spectroscopic challenge. The interaction of the singlet and triplet Rydberg states with the ion-pair potentials for energies > 72,000 cm^{-1} should be an interesting area for future study. As already mentioned, experimental measurement of radiative lifetimes and radiative branching ratios would be useful and much remains to be learned about the spectroscopy of ClF from application of the OODR method.

Now that the $A'(^3\Pi_2)$, $A(^3\Pi_1)$ and $B(^3\Pi_{0^+})$ states are fully characterized, collisional processes among these nested states can be studied in which a given vibrational-rotational state is prepared and monitored in time by various types of OODR experiments. The addition of a second probe laser would enable product states to be monitored simultaneously. Since $\omega_e \approx 360$ cm^{-1}, the vibrotational levels are easily resolved and state-to-state kinetic measurements are possible. In fact, we have acquired preliminary data for rotational relaxation measurements of $ClF(B^3\Pi_{0^+})$ in He and Ar bath gas.[39] In a qualitative sense, the vibrational and rotational relaxation rates for the $B(^3\Pi_{0^+})$ state seem to be normal for a diatomic molecule of this type. However, the electronic relaxation rates to the A and A' states probably are slow.

After the radiative lifetimes of the D', E, β, f and G states are established, collisional relaxation among individual vibrational levels of these ion-pair states also can be studied by observations of their time and wavelength resolved fluorescence. For example, we performed one quenching measurement by Xe for the thermally equilibrated D', E and β states using their integrated emission intensity. The Stern-Volmer plot of the Cl^+F^- emission intensity for Xe pressures of 5-25 Torr was linear and the slope ($k_{Xe}\tau$) was 4.2×10^{-18} cm^3 $molecule^{-1}$. The reactive quenching rate constants for ion-pair states are large and expected values are $3\text{-}5 \times 10^{-10}$ cm^3 $molecule^{-1}$ s^{-1}, which suggest an average radiative lifetime of 8-14 ns. With shorter pulse lasers, time resolved measurements of the collision dynamics of the ClF ion-pair states are possible.

Acknowledgment. The work at Kansas State University was supported by the US National Science Foundation (Grant CHE-9505032). We thank Dr. J. Tellinghuisen for his important collaborative effort with the experimental spectroscopy of ClF. We also thank the authors of reference 8 and 9 for sharing the results of their *ab initial* calculations. We especially wish to thank Dr. D. Koch for assistance with the bound-free computations.

References

1. Coxon, J. A. In *Molecular Spectroscopy*; Barrow, R. F., Long, D. A., Miller, D. J., Eds.; Specialist Periodical Reports; The Chemical Society: 1973; Vol 1, p 177.
2. Heaven, M. C. *Chem. Soc. Rev.* **1986**, *15*, 405.
3. Brand, J. C. D.; Hoy, A. R. *Appl. Spectroscopy Reviews* **1987**, *23*, 285.
4. Alekseev, V. A.; Setser, D. W. *J. Chem. Phys.* **1997**, *107*, 4771.
5. Kokh, D. B.; Alekseev, V. A.; Setser, D. W. *J. Chem. Phys.* **1998**, *109*, 1763.
6. Alekseev, V. A.; Setser, D. W.; Tellinghuisen, J. *J. Mol. Spectrosc.* **1999**, *194*, 61.
7. Alekseev, V. A.; Setser, D. W.; Tellinghuisen J. *J. Mol. Spectrosc.* **1999**, *195*, 162.
8. Alekseev, A. B.; Libermann, H.-P.; Buenker, R. J.; Kokh, D. B. *J. Chem. Phys.* **1999**, In press.
9. Alekseev, V. A.; Kokh, D. B.; Setser, D. W.; Alekseev, A. B.; Libermann, H.-P.; Buenker, R. J. 2000, to be published.
10. Darvesh, K.; Boyd, R. J.; Peyerimhoff, S. D. *Chem. Phys.* **1988**, *121*, 361.
11. Coxon, J. A. *Chem. Phys. Lett.* **1975**, *33*, 136. Since the dissociation limit of $ClF(B^3\Pi_{0^+})$ has been established[4] as $Cl(^2P_{3/2}) + F(^2P_{1/2})$, the bond energy question has been settled in favor of the higher value.
12. Ishiwata, T.; Kasai, Y.; Obi, K. *J. Chem. Phys.* **1991**, *95*, 60.
13. Diegelmann, M.; Hohla, K.; Rebentrost, F.; Kompa, K. L. *J. Chem. Phys.* **1982**, *76*, 1233.
14. Diegelmann, M.; Proch, D.; Zensheng, Z. *Appl. Phys. B* **1986**, *40*, 49.
15. Walter, W.; Laughghoff, H.; Sauerbrey, R. *Appl. Phys. B* **1984**, *35*, 11.
16. Alberti, F.; Huber, K. P.; Looi, E. C. *J. Molec. Spectrosc.* **1983**, *102*, 289.

17. (a) Worner, J.; Moller, T.; Stapelfeldt, J.; Zimmer, G.; Haaks, D.; Kampf, S.; Le Calve', J.; Castex, M. C. *Z. Phys. D* **1988**, *D7*, 383. (b) Moller, T.; Jordan, B.; Gurtler, P.; Zimmerer, G.; Haaks, D.; Le Calve', J.; Castex, M. *Chem. Phys.* **1983**, *76*, 295. (c) Li, L.; Lipert, R. J.; Park, H.; Chupka, W.; Colson, S. D. *J. Chem. Phys.* **1988**, *88*, 4608. (d) Yamanouchi, K.; Tsuchizawa, T.; Miyawaki, J.; Tsuchiya, S. *Chem. Phys. Lett.* **1989**, *156*, 301. (e) Tsukiyama, K.; Kuramatsu, Y.; Tsukakoshi, M.; Misu, M.; Kasuya, T. *Chem. Phys. Lett.* **1988**, *152*, 523.
18. (a) Wang, P.; Dimov, S. S.; Rosenblood, G.; Lipson, R. H. *J. Phys. Chem.* **1995**, *99*, 3984. (b) Al-Kahali, M. S. N.; Donovan, R. J.; Lawley, K. P.; Redley, T.; Yarwood, A. J. *J. Phys. Chem.* **1995**, *99*, 3978. (c) Al-Kahali, M. S. M.; Donovan, R. J.; Lawley, K. P.; Min, Z.; Ridley, T. *J. Chem. Phys.* **1996**, *104*, 825. (d) Al-Kahali, M. S. N.; Donovan, R. J.; Lawley, K. P.; Ridley, T. J. *Chem. Phys.* **1996**, *104*, 1833.
19. Peyerimhoff, S. D.; Buenker, R. J. *Chem. Phys.* **1981**, *57*, 279.
20. (a) Shinzawa, T.; Tokunaga, A.; Ishiwata, T.; Tanaka, I. *J. Chem. Phys.* **1985**, *83*, 5407. (b) Ishiwata, T.; Shinzawa, T.; Kusayanogi, T.; Tanaka, I. *J. Chem. Phys.* **1985**, *82*, 1788. (c) Ishiwata, T.; Si, J.-H.; Obi, K. *J. Chem. Phys.* **1992**, *96*, 5678.
21. (a) Ishiwata, T.; Kasai, Y.; Obi, K. *J. Chem. Phys.* **1993**, *98*, 3620. (b) Si, J.-H.; Ishiwata, T.; Obi, K. *J. Mol. Spectrosc.* **1991**, *147*, 334.
22. (a) Ishiwata, T.; Hara, T.; Obi, K.; Tanaka, I. *J. Chem. Phys.* **1987**, *87*, 2513. (b) Ishiwata, T.; Obi, K.; Tanaka, I. *J. Phys. Chem.* **1991**, *95*, 2763.
23. (a) Ishiwata, T.; Obi, K.; Tanaka, I. *J. Mol. Spectrosc.* **1988**, *127*, 353. (b) Ishiwata, T.; Ishiguro, A.; Obi, K. *J. Mol. Spectrosc.* **1991**, *147*, 300, 321.
24. Stricker, W.; Krauss, L. *Z. Naturforsch.* **1968**, *A23*, 1116.
25. (a) McDermid, I. S. *J. Chem. Soc., Faraday Trans. 2* **1981**, *77*, 519. (b) McDermid, I. S.; Laudenslanger, J. B. *Chem. Phys. Lett.* **1981**, *79*, 370.
26. (a) Tellinghuisen, P. C.; Guo, B.; Chakraborty, D. K.; Tellinghuisen, J. *J. Mol. Spectrosc.* **1988**, *128*, 268. (b) Radzykewycz, D. T.; Littlejohn, C. D.; Carter, M. Brian; Clevenger, J. O.; Tellinghuisen, J. *J. Mol. Spectrosc.* **1994**, *166*, 287.
27. (a) Brand, J. C. D.; Hoy, A. R.; Risbud, A. C. *J. Mol. Spectrosc.* **1985**, *113*, 47. (b) Brand, J. C. D.; Hoy, A. R.; Jaywant, S. M. *J. Mol. Spectrosc.* **1984**, *106*, 388. (c) Brand, J. C. D.; Deshpande, U. D.; Hoy, A. R.; Jaywant, S. M. *J. Mol. Spectrosc.* **1983**, *100*, 416.
28. (a) Narayani, R. I.; Tellinghuisen, J. *J. Mol. Spectrosc.* **1990**, *141*, 79. (b) Zhang, X.; Heaven, M. C.; Tellinghuisen, J. *J. Mol. Spectrosc.* **1994**, *144*, 135. (c) Brown, S. W.; Dowd, C. J. Jr.; Tellinghuisen, J. *J. Mol. Spectrosc.* **1988**, *132*, 178.
29. (a) Ishiwata, T.; Shinzawa, T.; Si, J.-H.; Obi, K.; Tanaka, I. *J. Mol. Spectrosc.* **1994**, *166*, 321. (b) Ishiwata, T.; Kusayanagi, T.; Tanaka, I. *J. Mol. Spectrosc.* **1995**, *173*, 552. (c) Ishiwata, T.; Kasai, Y.; Obi, K. *Chem. Phys. Lett.* **1966**, *261*, 175.
30. Cohen, J. S.; Schneider, B. *J. Chem. Phys.* **1974**, *61*, 3230.
31. Clyne, M. A. A.; Martinez, E. *J. Chem. Soc., Faraday Trans. 2* **1980**, *76*, 1275, 1651.
32. Heaven, M. C.; Clyne, M. A. A. *J. Chem. Soc., Faraday Trans. 2* **1982**, *78*, 1339.
33. van de Burgt, L. J.; Heaven, M. C. *Chem. Phys.* **1986**, *103*, 407.
34. (a) Wolf, P. J.; Glover, L.; Shea, R. F.; Davis, S. J. *J. Chem. Phys.* **1985**, *82*, 2321. (b) Wolf, D. J.; Davis, S. J. *J. Chem. Phys.* **1985**, *83*, 91.
35. Perram, G. P.; Davis, S. J. *J. Chem. Phys.* **1990**, *93*, 1720.
36. van de Burgt, L. J.; Heaven, M. C. results quoted in ref. 2.
37. Coombe, R. D.; Pilipovich, D.; Horne, R. K. *J. Phys. Chem.* **1978**, *82*, 2284.
38. Nelson, T. O.; Setser, D. W.; Qin, J. *J. Phys. Chem.* **1993**, *97*, 2585.
39. Alekseev, V. A. **1999**, unpublished work.
40. Bibinov, N. K.; Davydov, V. K.; Fateev, A. A.; Kokh, D. B.; Lugovoj, E. V.; Ottinger, Ch.; Pravilov, A. M. *J. Chem. Phys.* **1998**, *109*, 10864.
41. Ishiwata, T.; Takekawa, H.; Obi, K. *Chem. Phys.* **1993**, *177*, 303.